Metabolic Engineering Communications 19 (2024) e00246

Contents lists available at ScienceDirect

Metabolic Engineering Communications

journal homepage: www.elsevier.com/locate/mec

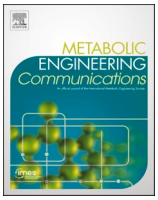

# Engineering thioesterase as a driving force for novel itaconate production via its degradation scheme

Ryan S. Wang, Siang-Wun Siao, Jessica C. Wang, Patrick Y. Lin, Claire R. Shen *

*Department of Chemical Engineering, National Tsing Hua University, 101, Section 2, Kuang-Fu Road, Hsinchu, 30013, Taiwan*

ARTICLE INFO

*Keywords:*
Itaconate
Driving force
Thioesterase
CoA hydrolysis
Metabolic engineering

ABSTRACT

Incorporation of irreversible steps in pathway design enhances the overall thermodynamic favorability and often leads to better bioconversion yield given functional enzymes. Using this concept, here we constructed the first non-natural itaconate biosynthesis pathway driven by thioester hydrolysis. Itaconate is a commercially valuable platform chemical with wide applications in the synthetic polymer industry. Production of itaconate has long relied on the decarboxylation of TCA cycle intermediate cis-aconitate as the only biosynthetic route. Inspired by nature's design of itaconate detoxification, here we engineered a novel itaconate producing pathway orthogonal to native metabolism with no requirement of auxotrophic knock-out. The reversed degradation pathway initiates with pyruvate and acetyl-CoA condensation forming (S)-citramalyl-CoA, followed by its dehydration and isomerization into itaconyl-CoA then hydrolysis into itaconate. Phenylacetyl-CoA thioesterase (PaaI) from *Escherichia coli* was identified via screening to deliver the highest itaconate formation efficiency when coupled to the reversible activity of citramalate lyase and itaconyl-CoA hydratase. The preference of PaaI towards itaconyl-CoA hydrolysis over acetyl-CoA and (S)-citramalyl-CoA also minimized the inevitable precursor loss due to enzyme promiscuity. With acetate recycling, acetyl-CoA conservation, and condition optimization, we achieved a final itaconate titer of 1 g/L using the thioesterase driven pathway, which is a significant improvement compared to the original degradation pathway based on CoA transferase. This study illustrates the significance of thermodynamic favorability as a design principle in pathway engineering.

## 1. Introduction

Engineering driving forces for a biosynthetic pathway is crucial in order to achieve higher carbon flux into the target product. Inefficient reactions often originate from suboptimal enzyme solubility, catalytic kinetics and cofactor supply. These challenges can sometimes be addressed by rigorous bioprospecting, increasing substrate concentration, fine-tuning of enzyme expression, and engineering cofactor promiscuity. However, when a pathway is inherently reversible or thermodynamically unfavorable, the effect of aforementioned approaches becomes limited and design of synthetic driving forces is necessary to push carbon flux toward the desired direction. Such driving forces often rely on coupling growth pressure to product formation such as redox balance in the case of 1-butanol production via reversed β-oxidation (Shen et al., 2011). In other cases, rerouting the biochemical pathway with irreversible steps can also enhance the overall pathway thermodynamic favorability and enable better bioconversion yields. Reactions such as decarboxylation (Atsumi et al., 2008b), deamination (Huo et al., 2011), and ATP or PEP hydrolysis (Lan and Liao, 2012; Lan and Wei, 2016) exhibit significantly negative $\Delta G'^{\circ}$ and were demonstrated in many studies to help irreversibly drive the flux forward when incorporated into the target pathway. Similarly, hydrolysis of a thioester bond provides thermodynamic driving force via the considerable energy drop and is synthetically introduced in this study to reverse the direction of the itaconate degradation pathway for use in biosynthesis.

Here, we demonstrated reversal of the itaconate catabolic pathway for itaconate production by installing an irreversible thioester hydrolysis step in place of the original CoA transfer (Fig. 1). Itaconate is a commercially valuable platform chemical with wide applications in the synthetic polymer industry (Corma et al., 2007; Okabe et al., 2009). Production of itaconate has long relied on the decarboxylation of TCA cycle intermediate cis-aconitate, forming the methylene-attached dicarboxylic acid with one carbon lost in the process. Despite its success in the native producers, the complex life cycle of fungi and the desire for additional traits such as photosynthetic biosynthesis have led to numerous efforts in engineering the fungal pathway in recombinant

* Corresponding author.
*E-mail address:* crshen@mx.nthu.edu.tw (C.R. Shen).

https://doi.org/10.1016/j.mec.2024.e00246
Received 15 June 2024; Received in revised form 31 July 2024; Accepted 2 August 2024
Available online 5 August 2024

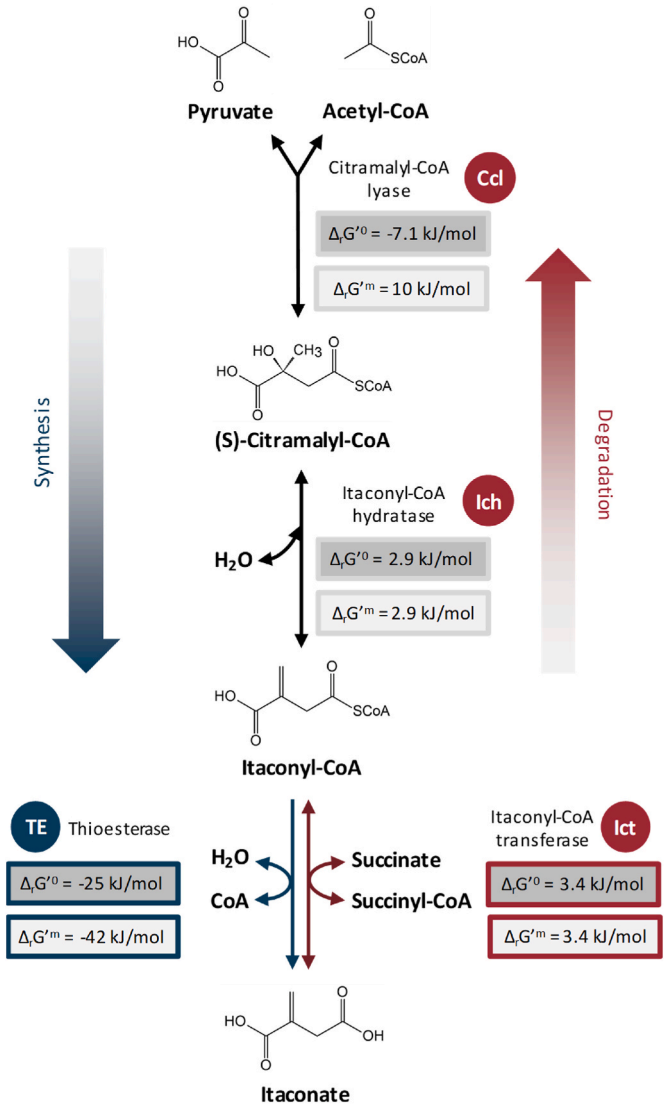


**Fig. 1.** Schematics of the thioesterase driven production of itaconate using its degradation pathway. The standard change in Gibbs free energy ($\Delta_rG'^{o}$) for each step in the itaconate synthesizing direction was calculated using eQuilibrator (Flamholz et al., 2012) and shown in the gray box. Also shown as $\Delta_rG'^{m}$ is the change in Gibbs free energy at substrate concentration of 1 mM calculated by eQuilibrator, which is likely closer to the intracellular state compared to the 1M in the standard case. Abbreviation of each enzyme is shown in the filled circle. Conditions for eQuilibrator calculations were set to pH 7.5 and ionic strength of 0.25M.

hosts. The insolubility of fungal cis-aconitate decarboxylase (Jeon et al., 2016; Otten et al., 2015) and necessity of TCA cycle disruption (Harder et al., 2018; Lu et al., 2021) often post challenges to the recombinant strain development and operation cost. The inevitable loss of cis-aconitate to the reversible interconversion of citrate and isocitrate also adds to the difficulty of securing precursor supply, which was recently tackled by replacing the native aconitase with the engineered dehydratase (Ye et al., 2022). Since no alternative biochemical pathway has been proposed and constructed for itaconate biosynthesis, we took interest in nature's design of itaconate degradation and set out to reverse its reaction sequence via engineering means (Fig. 1). Itaconate detoxification pathway had evolved in certain infectious bacteria such as *Yersinia pestis*, *Pseudomonas aeruginosa*, and *Burkholderia xenovorans* to combat the growth suppression caused by the itaconate inhibition of the glyoxylate shunt and the methylcitrate cycle (Ruetz et al., 2019; Sasikaran et al., 2014). During infection, the natural defense mechanism of mammalian macrophage works through the synthesis and release of itaconate (Luan and Medzhitov, 2016; Michelucci et al., 2013), which allosterically inactivates isocitrate and methylcitrate lyase and disables the pathogen's ability to assimilate acetyl-CoA or propionyl-CoA in the glucose limiting condition. Degradation of itaconate initiates with CoA activation of the dicarboxylic acid via itaconyl-CoA transferase (Ict). The resulting itaconyl-CoA is then converted into (S)-citramalyl-CoA via itaconyl-CoA hydratase (Ich) possessing both the itaconyl-CoA isomerase and mesaconyl-CoA hydratase activity module. Lastly, cleavage of (S)-citramalyl-CoA into acetyl-CoA and pyruvate occurs through the action of (S)-citramalyl-CoA lyase (Ccl), which has homologues commonly found in the 3-hydroxypropionate cycle (Zarzycki et al., 2009).

Inspired by the reversal of β-oxidation pathway via fermentative NADH balance for 1-butanol production (Shen et al., 2011), we attempted at creating a synthetic driving force to push carbon flow in the itaconate synthesis direction using the thermodynamically favorable thioester hydrolysis. The use of acyl transfer potential to drive biochemical reactions is commonly found in metabolism. The lower efficiency at resonance stabilization of thioesters results in a greater energy drop from its hydrolysis than the analogous oxygen esters. By substituting the last CoA-transfer step ($\Delta_rG'^{o} = 3.4$ kJ/mol) with CoA hydrolysis ($\Delta_rG'^{o} = -25$ kJ/mol) using thioesterase (Fig. 1), the inherently reversible itaconate degradation pathway with an overall $\Delta G'^{o}$ of −0.8 kJ/mol was transformed into a thermodynamically favorable pathway with an overall $\Delta G'^{o}$ of −29.2 kJ/mol. It is noted that the drop in Gibbs free energy for itaconyl-CoA hydrolysis is even greater when the substrate concentration is set to 1 mM (Flamholz et al., 2012), a level more appropriate physiologically to describe the intracellular metabolites. Acyl-CoA thioesterase belongs to a broad superfamily of thioester hydrolases which catalyze the cleavage of thioester bond of metabolic intermediates found in many essential pathways such as fatty acid and steroid biosynthesis, β-oxidation, and mevalonate metabolism (Swarbrick et al., 2020). The wide range of reactions participated thus makes acyl-CoA thioesterase possess a stellar spectrum of substrate range, covering but not limited to saturated/unsaturated fatty acyl-CoA, methyl-branched acyl-CoA, aromatic acyl-CoA, and carboxylic acyl-CoA (Cantu et al., 2010). The diverse function and structure of thioesterases also make classification difficult; currently the acyl-CoA thioesterases are roughly categorized by their sequence homology, structural domain, and catalytic mechanism (Tillander et al., 2017), with type I being in the α/β-hydrolase protein family and type II having the signature "hotdog" fold motif. As revealed by many studies, type II acyl-CoA thioesterases typically exhibit broader substrate promiscuity (Kotowska and Pawlik, 2014; McMahon and Prather, 2014; Ohlemacher et al., 2018) due to the absence of a well-conserved substrate binding pocket (Zhuang et al., 2008), thus allowing them to participate in a wide array of reactions with divergent functions.

In this work, we engineered the first non-natural itaconate producing pathway driven by thioester hydrolysis. Identification of proper thioesterase with itaconyl-CoA activity was the key factor in reversing the itaconate degradation pathway for biosynthesis. The low preference of target thioesterase towards pathway precursors acetyl-CoA and (S)-citramalyl-CoA was also important to minimize undesired substrate competition and prevent precursor loss. Although the achieved titer and yield are still low compared to the current itaconate production route, our proposed pathway inherently possesses higher energy efficiency that may serve as an attractive trait once fully enhanced. Compared to the natural fungi pathway which generates 1 mol of ATP for every mole of glucose converted to itaconate, the reversed degradation pathway makes 2 mol of ATP due to the distinctive pathway feature (for detailed reaction balance, see Supplementary Fig. 1). The maximum theoretical yield and NADH balance remain the same between the two pathways. While still at its early developmental stage, this study demonstrates a proof-of-concept design of synthetic itaconate pathway based on thermodynamic favorability. The engineering principle and novel itaconate

pathway presented here should be readily transferable to other production systems and recombinant hosts.

## 2. Results and discussion

### 2.1. Assessment of itaconate production via its catabolic enzymes

To examine the inherent possibility of itaconate accumulation via its degradation pathway, we first surveyed the enzyme candidates from the natural itaconate degrading microorganisms (Sasikaran et al., 2014). Genes encoding for the citramalyl-CoA lyase (Ccl), itaconyl-CoA hydratase (Ich), and itaconyl-CoA transferase (Ict) from *Yersinia pseudotuberculosis* (Yp), *Pseudomonas aeruginosa* (Pa) and *Burkholderia xenovorans* (Bx) were cloned and overexpressed in *E. coli* along with a few other homologues identified by protein blast and bioprospecting. Ict from *Salmonella enterica serovar typhimurium* was selected as an alternative candidate based on its similar pathogenicity and the 76% protein identity with YpIct. Malyl-CoA lyase from *Rhodobacter capsulatus* (RcCcl), which naturally catalyzes the reversible condensation of glyoxylate and acetyl-CoA or propionyl-CoA (Meister et al., 2005), was also tested for its potential unspecific activity towards pyruvate. Based on the thermodynamics calculation of each reaction using the eQuilibrator (Flamholz et al., 2012), the overall Gibbs free energy change of the itaconate catabolic pathway is very close to neutral with no natural push in the synthesis direction (Fig. 1). Even when all three enzymes are functioning effectively, itaconate formation might be challenging to observe intracellularly without a kinetic trap, especially under strong competition of pyruvate and acetyl-CoA by other essential reactions. Detoxification of itaconate using this pathway was reported to be extremely efficient where high level of itaconate can be degraded with just a catalytic amount of CoA ester (Sasikaran et al., 2014). In the case of YpIct which displays relaxed CoA ester specificity, itaconate can be effectively activated by acetyl-CoA, propionyl-CoA, and butyryl-CoA in addition to the natural co-substrate succinyl-CoA (Sasikaran et al., 2014). The ability to use acetyl-CoA, the end product of itaconate detoxification, as the CoA donor for next round of itaconate activation circumvents the need of fresh succinyl-CoA supply and further strengthens pathway efficiency in the degradation direction.

To assess the possibility of itaconate production via the degradation enzymes, *in vitro* biosynthesis of itaconate using purified enzymes was first performed to ensure functional expression of each enzyme and allow saturating concentration of the precursors pyruvate and acetyl-CoA. Different combinations of the bioprospected enzyme homologues were then sequentially checked based on their itaconate formation efficiency. As shown on Fig. 2A, the highest accumulation of itaconate *in vitro* was achieved by YpCcl, PaIch, and YpIct, reaching nearly 10 mg/L in 30 min. Other homologue combinations led to 10–80% lower level of itaconate formation with RcCcl performing the worst, suggesting its low substrate preference towards pyruvate. Next, to further examine the potential of accumulating itaconate based on the intracellular concentration of pyruvate and acetyl-CoA, we cloned the best performing enzymes into an operon (PaIch-YpCcl-YpIct, plasmid pSW41) and attempted itaconate synthesis *in vivo* by overexpressing this catabolic pathway in the fermentation deleted strain JCL299 (Δ*ldhA* Δ*adhE* Δ*frdBC* Δ*pta*). Elimination of fermentative reactions was consistently shown to improve biochemical productions derived from pyruvate and/or acetyl-CoA such as isobutanol (Atsumi et al., 2008b), 1-butanol (Shen et al., 2011), and 2,3-butanediol (Liang and Shen, 2017). In our case, use of JCL299 allowed approximately four-fold higher level of itaconate formation (~8 mg/L) compared to the titer achieved using wild type *E. coli*. As one can see from Fig. 2, similar level of itaconate production was observed *in vitro* and *in vivo* with addition of succinate as the essential co-substrate for the itaconyl-CoA transferase. This observation indicates the sufficiency of intracellular pyruvate and acetyl-CoA concentration to direct carbon flux into itaconate via the highly reversible pathway. The low accumulation of itaconate, however, in both the *in vivo* and *in vitro* cases appeared to have originated from the pathway reversibility and a lack of driving force. Design of a synthetic push to further drive carbon flux into the target itaconate is thus pursued next.

### 2.2. Screening of thioesterases to drive itaconate production

In previous studies, accumulation of NADH (Shen et al., 2011) and pathway rewiring with ATP dependent reactions (Lan and Liao, 2012) have successfully channeled carbon flux towards 1-butanol production via the highly reversible β-oxidation pathway. However, the itaconate

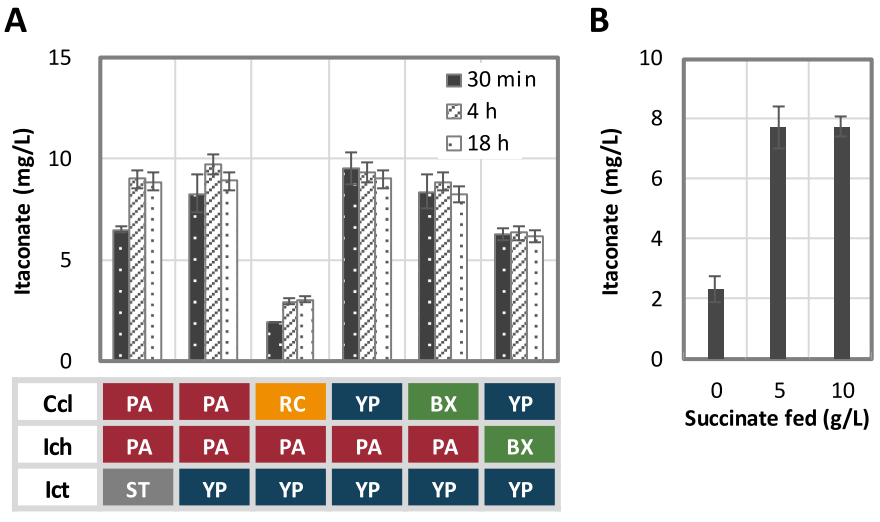


**Fig. 2.** Assessment of itaconate performance via its catabolic enzymes. (A) *In vitro* verification and comparison of different enzyme candidates found in the itaconate degradation pathway. Purified enzymes were used in various combinations for *in vitro* itaconate synthesis. Enzyme sources were abbreviated and color coded as show in the table below. (B) *In vivo* production of itaconate using YpCcl, PaIch, and YpIct. Strain JCL299 (Δ*ldhA* Δ*adhE* Δ*frdBC* Δ*pta*) was transformed with plasmid pSW41 and allowed to produce for 48 h with or without supplementation of succinate. Error bars represent standard deviation of three duplicates. PA, *Pseudomonas aeruginosa*; YP, *Yersinia pseudotuberculosis*; BX, *Burkholderia xenovorans*; ST, *Salmonella enterica serovar typhimurium*; RC, *Rhodobacter capsulatus*; Ccl, citramalyl-CoA lyase; Ich, itaconyl-CoA hydratase; Ict, itaconyl-CoA transferase. (For interpretation of the references to color in this figure legend, the reader is referred to the Web version of this article.)

degradation pathway does not exhibit any cofactor or redox dependency nor nutrition auxotrophic characteristics that can be directly implemented as driving force. Since metabolic pathways found in nature such as fatty acid biosynthesis are often driven by the acyl transfer potential, substitution of CoA transferase with thioesterase should provide an effective kinetic trap to irreversibly push carbon into itaconate. Since no thioesterase has been specifically characterized for itaconyl-CoA activity, here we bioprospected for endogenous thioesterases in *E. coli* for their ease of expression and potential substrate promiscuity. Elimination of native thioesterase is often reported to be necessary to minimize unspecific hydrolysis of CoA intermediates into acid byproducts (Shen et al., 2017). In addition to the ones involved in fatty acid biosynthesis, *E. coli* possesses a wide range of thioesterases with unclear physiological function. A total of 17 enzymes (FadM, YdiI, YciA, YbgC, YbfF, YpfH, TesA, TesB, YbaC, YjfP, BioH, YbdB, FrsA, PaaI, PaaY, YeiG, YqiA) annotated or reported with thioesterase activity was selected (Shen et al., 2017) along with (3S)-malyl-CoA thioesterase (Mcl2) from *Rhodobacter sphaeroides* for its potential activity towards itaconyl-CoA (Erb et al., 2010). Strain JCL299 harboring plasmids pIA1 ($P_L$lac01:PaIch-YpCcl) and the different thioesterases overexpressed from pBR302 backbone was cultivated under microaerobic condition, and the resulting itaconate formation was compared. As shown on Fig. 3A, nearly all thioesterase candidates demonstrated certain degree of hydrolytic activity towards itaconyl-CoA as reflected by the 10–40 mg/L of itaconate secretion in 24 h. YpIct overexpressed from a similar backbone system as the thioesterases was used here as a negative control for comparison.

The thioesterases which delivered higher level of itaconate (>15 mg/L) were identified to be YciA, YbgC, YjfP and PaaI. It is interesting to note that three of the enzymes except YjfP belong to the type II thioesterase class which was demonstrated to exhibit broad substrate activity. Of the two highest itaconate producing thioesterases, YciA was reported to possess a wide spectrum of substrate promiscuity ranging from short-chain (such as acetyl-CoA, isobutyryl-CoA) and long chain (such as *n*-decanoyl-CoA, oleoyl-CoA) aliphatic acyl-CoA to phenyl acyl-CoA substrates (Zhuang et al., 2008). On the other hand, PaaI found in the phenylacetate degradation pathway is generally considered to hydrolyze phenylacetyl-CoA and its mono- and di-hydroxy ring analogues, rather than aliphatic acyl-CoA thioesters (Song et al., 2006). To further confirm the superior performance of PaaI, itaconate productions using thioesterase PaaI and YciA were repeated under optimized cultivation condition and pH adjustment, with the CoA transferase YpIct as control comparison (Fig. 3B). It is noted that the redox neutral property of the reversed itaconate degradation pathway puts oxygen demand at a challenging position. Lower supply of oxygen is typically ideal to maintain higher pool of acetyl-CoA and pyruvate in the fermentation deleted strain (JCL299). However, the need to recycle reducing power in JCL299 makes respiration essential. As shown on Fig. 4, preliminary assessment of ideal aeration level by varying cultivation vessel and liquid volume indicated that microaerobicity (20 mL culture in 125 mL non-baffled screw cap flask) enabled the best itaconate production. On the other hand, oxygen supply on the extreme ends (fully aerated in baffled flasks or minimal aeration in sealed tubes) resulted in significantly lower accumulation of itaconate. At last, implementation of the optimal aeration and pH adjustment greatly elevated itaconate formation to 150 mg/L in 48 h using PaaI (Fig. 3B), which was about four and 15 fold higher than the amount achieved by YciA and the transferase YpIct respectively.

### 2.3. Kinetic analysis of thioesterase PaaI for the CoA intermediates in the itaconate pathway

As reported in prior studies, many type II thioesterases possess unspecific activity toward a wide range of acyl-CoA substrates. Since the itaconate degradation pathway involves three different acyl-CoA intermediates, namely acetyl-CoA, (S)-citramalyl-CoA, and itaconyl-CoA, we set out to characterize the thioesterase activity of our positive candidate PaaI towards each of the CoA substrates. Due to the unavailability of (S)-citramalyl-CoA and itaconyl-CoA commercially, we first pursued the *in vitro* preparation of these two CoA compounds by the itaconate degradation reactions. As shown by the HPLC chromatograms (Fig. 5), incubation of itaconate and acetyl-CoA with the CoA transferase YpIct or in combination with the hydratase PaIch resulted in the formation of distinct new peaks using the C18 column. Acetyl-CoA was used here as the CoA donor for its comparable efficiency as succinyl-CoA partnering with YpIct (Sasikaran et al., 2014). When only YpIct was present, the new peak around 15.5 min gradually enlarged while the acetyl-CoA peak shrunk with similar aspect ratio as time progressed from 0 to 30 min. Subsequent addition of PaIch after observation of the 15.5 min peak led to appearance of the 7.6 min peak with drop of the 15.5 min peak area. Based on the respective reaction sequence and peak behavior, we then identified the 15.5 min peak as itaconyl-CoA and the 7.6 min peak as (S)-citramalyl-CoA. The (S)-citramalyl-CoA peak was further confirmed by incubation of the citramalyl-CoA lyase YpCcl with pyruvate and acetyl-CoA, which resulted in the gradual appearance of the 7.6 min peak with consumption of acetyl-CoA.

With successful preparation and identification of the CoA intermediates, we proceeded with kinetic assay of the thioesterase PaaI. Contrary to the general observation of broad substrate range associated with type II thioesterases, PaaI displayed relatively low activity towards itaconyl-CoA (0.17 U/mg, U: μmol/min) and even lower activity

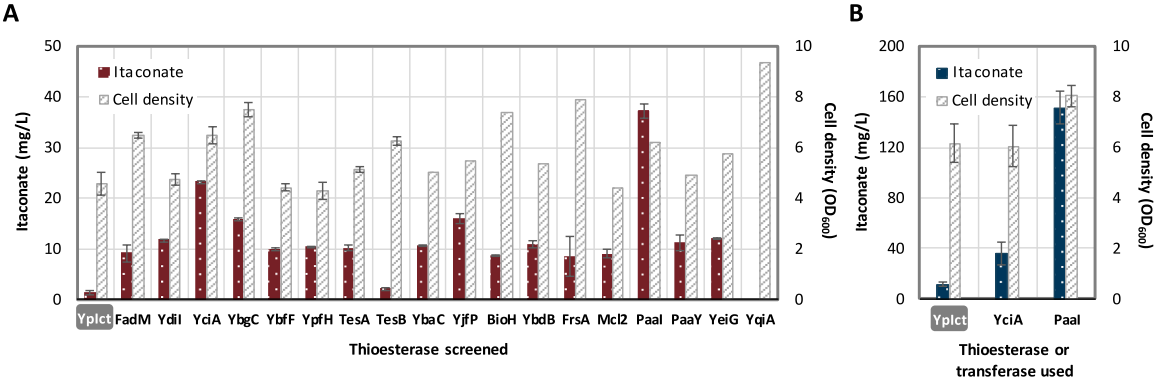


**Fig. 3.** Screening of thioesterase to drive itaconate biosynthesis. (A) Strain JCL299 (Δ*ldhA* Δ*adhE* Δ*frdBC* Δ*pta*) was co-transformed with plasmids pIA1 and pSW32 (harbouring YpIct as negative control), or pIA1 and ASKA plasmids containing the corresponding thioesterase genes. Samples were taken after 24 h of cultivation. (B) Confirmation and comparison of the two best positive thioesterases on itaconate production at 48 h using optimized cultivation condition (glucose feeding and pH adjustment every 12 h, see Methods). Same transformed strains as (A) were used. Error bars represent standard deviation of three duplicates.

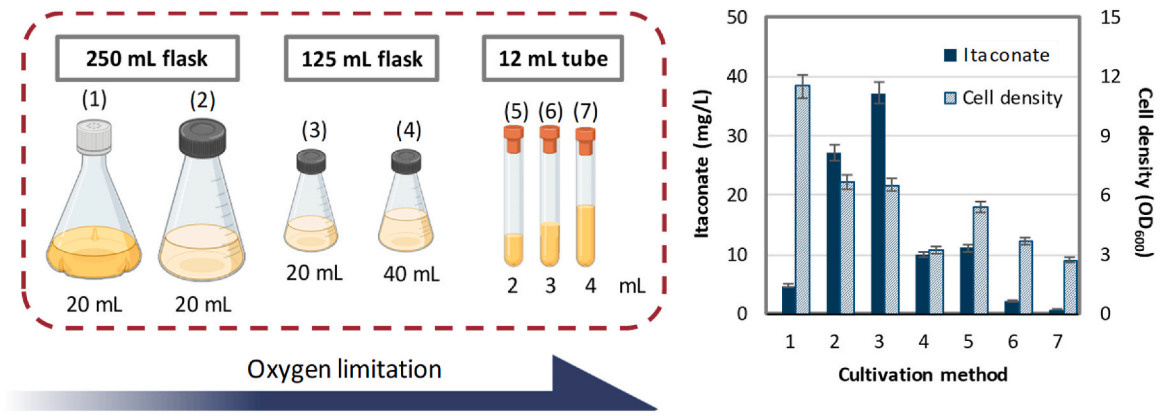


**Fig. 4.** Preliminary assessment of ideal aeration level by varying cultivation vessel and liquid volume. Left panel shows the cultivation set-up with method labels (1) to (7), corresponding to the x-axis on the graph. For detailed procedure, see Methods. Strain JCL299 (Δ*ldhA* Δ*adhE* Δ*frdBC* Δ*pta*) transformed with plasmids pIA1 and pASKA-*paaI* was used here. Samples were taken after 24 h of incubation. Error bars represent standard deviation of three duplicates.

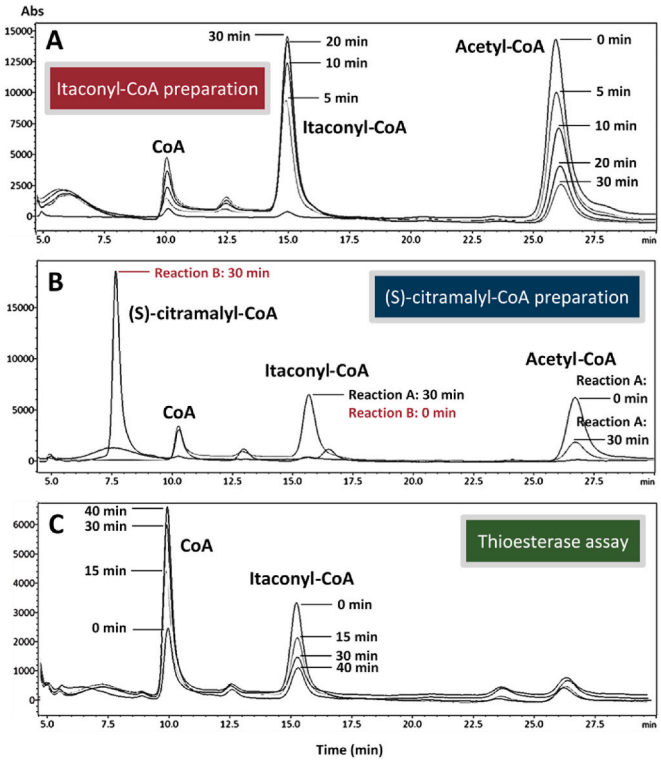


**Fig. 5.** HPLC preparation and analysis of the CoA thioesters. (A) Itaconate and acetyl-CoA were incubated with YpIct for 30 min to form itaconyl-CoA. (B) Following itaconyl-CoA formation by reaction shown in (A), PaIch was added to the reaction mixture for 30 min to convert itaconyl-CoA into (S)-citramalyl-CoA. Incubation of acetyl-CoA and itaconate with YpIct and PaIch simultaneously resulted in equally high conversion of acetyl-CoA to (S)-citramalyl-CoA as the sequential reactions shown here and was chosen as the final synthesis method. (C) Incubation of thioesterase PaaI with itaconyl-CoA prepared from the reaction shown in (A).

towards acetyl-CoA (0.015 U/mg) compared to the level reported for its most active hydroxyphenylacetyl-CoA substrates (Song et al., 2006). In addition, no activity was detected towards the pathway intermediate (S)-citramalyl-CoA, which was also reflected by no accumulation of citramalate in the itaconate production broth. Based on our kinetics analysis, the (S)-citramalyl-CoA lyase YpCcl demonstrated suboptimal but higher activity towards acetyl-CoA compared to the level observed in PaaI (Table 1). This skewed preference of PaaI towards itaconyl-CoA

**Table 1**
Kinetic assay of *E. coli* PaaI and YpCcl towards different acyl-CoA substrates. 1U = 1 μmol/min.

| Enzyme | Substrate | Specific activity (U/mg) |
|---|---|---|
| **PaaI** | Acetyl-CoA | 0.015 ± 0.006 |
| | (S)-Citramalyl-CoA | ND |
| | Itaconyl-CoA | 0.17 ± 0.02 |
| **YpCcl** | Acetyl-CoA + Pyruvate | 0.06 ± 0.02 |

ND: Not detected.

over the other CoA intermediates in the pathway helped minimize loss of key precursors to unspecific hydrolysis and contributed significantly to the superior performance of PaaI in itaconate production. *E. coli* PaaI is hypothesized to have evolved from the same superfamily with the *Arthrobacter* 4-hydroxyphenacyl-CoA thioesterase. Structural and activity analysis (Song et al., 2006) revealed that it is functionally unrelated to the benzoate-based metabolic pathways and exhibits undetectable to minimal activity towards benzoyl-CoA and aliphatic acyl-CoA thioesters respectively. It is noted that extremely low activity towards C2 to C6 saturated aliphatic thioesters such as acetyl-CoA, butyryl-CoA, and hexanoyl-CoA was also observed from the *Arthrobacter* PaaI homologue (Song et al., 2006), along with methylmalonyl-CoA which structurally resembles itaconyl-CoA in terms of its carboxylated and methylated feature. Our finding of the relatively decent itaconyl-CoA activity from the *E. coli* PaaI thioesterase adds to the insight of its substrate spectrum. Itaconate production via this CoA-bound pathway should benefit greatly from the specificity of PaaI given that itaconyl-CoA activity can be elevated without lifting the limited activity towards the other CoA intermediates.

To attempt at improving *E. coli* PaaI activity towards the short chain unsaturated itaconyl-CoA, we survey the literature for potential protein design ideas. As shown previously by studies on PaaI structure and mechanism (Song et al., 2006), mutations of active site residues D16 and H52 modified *E. coli* PaaI activity towards various hydroxylated phenylacetyl-CoA, suggesting the key role of D16 and H52 in substrate binding and the thioesterase activity. Based on this observation, we performed saturated mutagenesis of D16 and H52 individually with the hope to identify PaaI mutants capable of delivering higher itaconate production efficiency. Unfortunately, as indicated by Supplementary Fig. 2, none of the PaaI variants led to better itaconate formation compared to the level achieved by the wild type PaaI; instead approximately three-fold lower itaconate titer was resulted by the mutations. It is possible that D16 and H52 surrounding the catalytic center contribute more in the overall thioester hydrolytic activity rather than substrate specificity. Considering the low structural similarity between

itaconyl-CoA and phenylacetyl-CoA (and the close itaconate titer demonstrated by each variant), single mutation in the catalytic center may not be sufficient to create significant change in the active site for such a distant substrate alteration. Further analysis of PaaI binding pocket and random mutagenesis will be pursued in the future to unlock additional key residues for activity enhancement towards itaconyl-CoA.

### 2.4. Acetate recycle and minimization

During the optimization of itaconate production, significant secretion of acetate was observed (>10 g/L), suggesting insufficiency of the reversed degradation pathway to sequester the high flux of pyruvate and acetyl-CoA. Similar amount of pyruvate was also noted in the production media. As mentioned previously, microaerobic cultivation was used here for itaconate biosynthesis to allow accumulation of precursors and NADH oxidation via respiration in the fermentation deleted strain JCL299. Examination of the (S)-citramalyl-CoA lyase (YpCcl) catalyzing the reversible condensation of pyruvate and acetyl-CoA revealed its relatively low activity (0.06 U/mg, Table 1) compared to the other endogenous competing reactions. The suboptimal reaction rate in the condensation direction thus might have contributed to the overflow of acetate. Limited supply of oxygen might further push the ATP-producing acetate formation which cannot be eradicated with just *pta* deletion.

Initially, elimination of citrate synthase (*gltA*) responsible for the entrance of TCA cycle was performed to conserve acetyl-CoA in the attempt to boost the condensation rate by YpCcl. However, itaconate level stayed the same. Since acetate excretion is commonly observed in *E. coli* fermentation due to metabolic overflow (De Mey et al., 2007), the most viable approach is to recycle the acetate back to acetyl-CoA. This should also help convert back any acetyl-CoA that was lost to acetate due to unspecific thioesterase activity present in the cell. Indeed, overexpression of the acetyl-CoA synthetase (Acs) led to a 30% increase in itaconate production; however, similar secretion level of acetate was observed. Further survey of literature (Clomburg et al., 2012) suggested that the highly-efficient promiscuous activity of the native thioesterase YciA towards acetyl-CoA often contributes to the accumulation of acetate. As shown by Fig. 6A, deletion of the endogenous YciA not only reduced acetate formation but also further enhanced itaconate production by 15% compared to the level achieved in strain JCL299. It is interesting to note that YciA was the second best candidate that led to better itaconate formation compared to the other endogenous thioesterases screened. The high activity of YciA towards acetyl-CoA can be a big disadvantage for the synthesis of itaconate using this CoA-bound pathway. It is thus essential to keep in mind that low preference for acetyl-CoA and the other CoA intermediates must be maintained while engineering thioesterases for better itaconyl-CoA activity.

### 2.5. Future prospects of the reversed itaconate degradation pathway

With the preliminary metabolic pathway tuning finished, we proceeded with condition optimization. From a series of aeration, pH, intermittent glucose feeding, and cell density testing (for detailed condition, see Methods), we achieved an itaconate titer of 1 g/L in 120 h, which is nearly 100-fold increase compared to the initial level obtained using the CoA transferase. Even though current production rate is still suboptimal, here we successfully demonstrated the effectiveness of installing a thermodynamic trap for setting the pathway direction. Relative to the irreversible thioester hydrolysis in the last step, the first two reactions may now become the limitation for the itaconate formation rate. Preliminary bottleneck analysis using *in vitro* assay of YpCcl coupled to PaIch showed that higher itaconyl-CoA and (S)-citramalyl-CoA synthesis rates were detected only when concentration of YpCcl

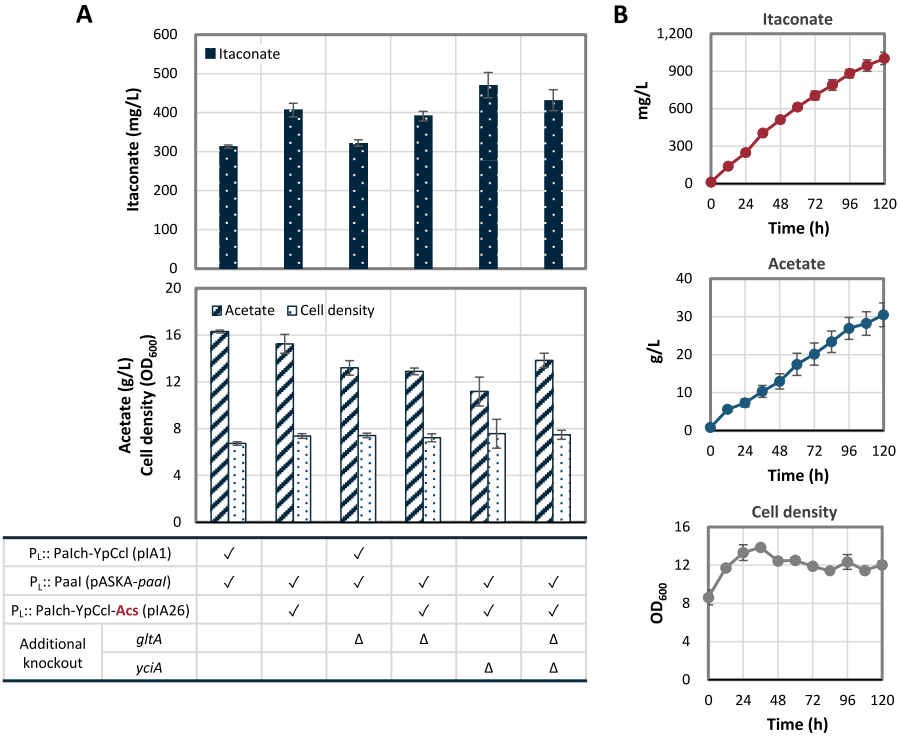


| | | | | | | | |
|---|---|---|---|---|---|---|---|
| $P_L$:: PaIch-YpCcl (pIA1) | | ✓ | | ✓ | | | |
| $P_L$:: PaaI (pASKA-*paaI*) | | ✓ | ✓ | ✓ | ✓ | ✓ | ✓ |
| $P_L$:: PaIch-YpCcl-**Acs** (pIA26) | | | ✓ | | ✓ | ✓ | ✓ |
| Additional knockout | *gltA* | | | Δ | Δ | | Δ |
| | *yciA* | | | | | Δ | Δ |

**Fig. 6.** Improving itaconate production by recycling acetate and minimizing acetate formation. (A) Different optimization strategies and their resulting itaconate formation at 96 h. Strain JCL299 (Δ*ldhA* Δ*adhE* Δ*frdBC* Δ*pta*) was used as the base strain, of which additional gene knock-outs are indicated by "Δ" in the table below. Cells transformed with the respective plasmids are labeled with "✓". Operon structure is shown next to the name of each plasmid. (B) Long term itaconate production using high cell density. Time indicates the time since cell concentration and resuspension into fresh medium. Error bars represent standard deviation of three duplicates.

increased and not affected by PaIch level (Supplementary Fig. 3). Overall, these observations suggest that in addition to PaaI activity optimization towards itaconyl-CoA, enhancing Ccl expression may also help boost the itaconate production efficiency in future study. Alternatively, reaction rewiring such as substituting the citramalyl-CoA lyase with citramalate synthase to synthesize citramalate as the pathway intermediate instead of citramalyl-CoA is another potential approach to further enhance itaconate forming efficiency given that a suitable dehydratase can be identified.

## 3. Conclusion

This work describes the design of a novel itaconate producing system driven by thioester hydrolysis, which has yet been reported in prior studies. By identifying the phenylacetyl-CoA thioesterase with itaconyl-CoA hydrolysis activity, we successfully rewired the itaconate detoxification pathway for itaconate biosynthesis. Compared to the natural fungal route via the TCA cycle, the proposed itaconate pathway exhibits the same maximum theoretical yield from glucose and identical redox balance. However, one additional mole of ATP is generated for every mole of itaconate synthesized from glucose using the reversed degradation pathway, which can be a beneficial trait during microbial biosynthesis. Although the present itaconate titer and yield are far below the traditional production level, the abundance of pyruvate and acetyl-CoA and decent expression of bacterial enzymes should grant the proposed pathway good potential for development in other unique hosts such as cyanobacteria or methanotrophs. Currently, the synthetic itaconate pathway appears to be mostly limited by the inefficient hydrolysis of itaconyl-CoA. Engineering thioesterases for better itaconyl-CoA activity while maintaining high specificity will thus be the next essential step to further improve itaconate production using this pathway.

## 4. Materials and Methods

### 4.1. Reagents and chemicals

All chemicals and reagents were purchased from Thermo Scientific (Pittsburgh, PA) or Sigma-Aldrich (Saint Louis, MO) unless otherwise specified. Taq DNA ligase, Phusion High-Fidelity DNA polymerase, and T5 exonuclease were obtained from New England Biolabs (Ipswich, MA). Oligonucleotides were purchased from IDT (San Diego, CA). KOD DNA polymerase was purchased from EMD Chemicals (San Diego, CA).

### 4.2. Bacteria strains and DNA manipulation

*Escherichia coli* BW25113 was designated as the wild type (Datsenko and Wanner, 2000). XL-1 Blue (Stratagene, La Jolla, CA) was used to propagate all plasmids. Construction of strain JCL16 (BW25113 with *lacI*$^q$ provided on F') and JCL299 was described in previous study (Atsumi et al., 2008a). All plasmids were created by the Gibson isothermal DNA assembly method (Gibson et al., 2009) using purified PCR fragments. A list of plasmids used is shown on Table 2. Except for the case of *E. coli* thioesterases which were obtained from the ASKA (A complete Set of *E. coli* K12 ORF Archive) plasmid library (Kitagawa et al., 2005), genes encoding for the Ict, Ich, Ccl, and thioesterase homologues were amplified from the corresponding genomic DNA purchased commercially: *Pseudomonas aeruginosa* (ATCC 47085D), *Yersinia pseudotuberculosis* (DSM 8992), *Burkholderia xenovorans LB400* (DSM 17367), *Salmonella enterica* subsp. *enterica* (DSM17058), *Rhodobacter capsulatus* (ATCC BAA-309), and *Rhodobacter sphaeroides* (DSM 5864). PaaI* D16 and H52 saturated variants were created using primers containing the mutated DNA sequence.

### 4.3. Cultivation medium and procedure for itaconate production

For all of the *in vivo* itaconate production and screening experiments, single colonies were picked from LB (Luria Broth) plates and inoculated into 2 mL of LB medium contained in test tubes with the appropriate antibiotics (kanamycin 50 μg/mL, spectinomycin 50 μg/mL and chloramphenicol 50 μg/mL). On the next day, the overnight culture grown at 37 °C was inoculated 1% (v/v) into 20 mL of terrific broth (TB) (12 g tryptone, 24 g yeast extract, 2.31 g $KH_2PO_4$, 12.54 g $K_2HPO_4$, 4 mL glycerol per liter of water) supplemented with 20 g/L of glucose and appropriate antibiotics in 125 mL screwed-cap flasks (PYREX 4985-125) unless otherwise noted. The culture was allowed to grow at 37 °C in a rotary shaker (250 rpm) to an $OD_{600}$ of 0.4–0.6 then induced with 0.1 mM IPTG and switched to 30 °C. Samples were taken and centrifuged to retrieve the supernatant throughout the production period. For itaconate productions using YpIct, 5 g/L of succinate was fed at the time of induction unless otherwise noted.

Identical medium and cultivation condition as described above were used in all of the figures except for the modifications outlined below. For Figs. 2B, 250 mL baffled flask (PYREX 4444-250) was used for the production cultivation. For Fig. 4, the inoculated cultures (1% v/v by overnight) were first grown in the 500 mL baffled flasks (PYREX 4444-500) at 37 °C in a rotary shaker (250 rpm) to an $OD_{600}$ of 0.4–0.6. Once reaching exponential phase, the cultures were induced with 0.1 mM IPTG and switched to 30 °C. After 4 h of induction at 30 °C, the induced cultures were then aliquoted to the different cultivation vessels as indicated on the figure for further itaconate production. The specific vessel product numbers are as follows: vessel 1 is PYREX 250 mL Delong Shaker Erlenmeyer Flask with Baffles (4444-250) with KIMBLE KIMKAP Polypropylene Cap (73660-38); vessel 2, 3, 4 are PYREX 250/

**Table 2**
Strains and plasmids used in this study.

| Strain | Genotype | Reference |
|---|---|---|
| BW25113 | *rrnB*$_{T14}$ Δ*lacZ*WJ16 *hsd*R514 Δ*araBAD*$_{AH33}$ Δ*rhaBAD*$_{LD78}$ | Datsenko and Wanner (2000) |
| XL-1 Blue | *recA1 endA1 gyrA96 thi-1 hsdR17 supE44 relA1 lac* [F′ *proAB lacI*$^q$ZΔ*M15 Tn10* (Tet$^R$)] | Stratagene |
| JCL 16 | BW25113/F' [*traD36*, *proAB*$^+$, *lacI*$^q$ZΔ*M15* (Tet$^r$)] | Atsumi et al. (2008a) |
| JCL 299 | JCL 16 Δ*ldhA* Δ*adhE* Δ*frdBC* Δ*pta* | Atsumi et al. (2008a) |
| JCY 298 | JCL299 Δ*gltA* | This study |
| JCY 299 | JCL299 Δ*yciA* | This study |
| JCY 399 | JCL299 Δ*yciA* Δ*gltA* | This study |
| **Plasmid** | **Genotype** | **Reference** |
| pSW26 | $P_{T5}$:: His6X-PaIch; pUC ori; Kan$^R$ | This study |
| pSW27 | $P_{T5}$:: His6X-PaIct; pUC ori; Kan$^R$ | This study |
| pSW28 | $P_{T5}$:: His6X-PaCcl; pUC ori; Kan$^R$ | This study |
| pSW29 | $P_{T5}$:: His6X-BxIch; pUC ori; Kan$^R$ | This study |
| pSW30 | $P_{T5}$:: His6X-BxCcl; pUC ori; Kan$^R$ | This study |
| pSW31 | $P_{T5}$:: His6X-StIct; pUC ori; Kan$^R$ | This study |
| pSW32 | $P_{T5}$:: His6X-YpIct; pUC ori; Kan$^R$ | This study |
| pSW33 | $P_{T5}$:: His6X-YpIch; pUC ori; Kan$^R$ | This study |
| pSW34 | $P_{T5}$:: His6X-YpCcl; pUC ori; Kan$^R$ | This study |
| pSW39 | $P_{T5}$:: His6X-RcCcl; pUC ori; Kan$^R$ | This study |
| pSW41 | $P_L$lacO1:: PaIch-YpCcl-YpIct; ColE1 ori; Amp$^R$ | This study |
| pIA1 | $P_L$lacO1:: PaIch-YpCcl; p15A ori; Spec$^R$ | This study |
| pIA16 | $P_{T5}$:: RsMcl2; pUC ori; Kan$^R$ | This study |
| pIA26 | $P_L$lacO1:: PaIch-YpCcl-*acs*; p15A ori; Spec$^R$ | This study |
| pASKA-TE[a] | $P_{T5\text{-}lac}$:: His6X-TE[a]; pBR322 ori; CM$^R$ | This study |
| pASKA-*paaI** [b] | $P_{T5\text{-}lac}$:: His6X-*paaI** [b]; pBR322 ori; CM$^R$ | This study |

Abbreviations indicate source of the genes: Pa, *Pseudomonas aeruginosa*; Bx, *Burkholderia xenovorans*; St, *Salmonella enterica serovar typhimurium*; Yp, *Yersinia pseudotuberculosis*; Rc, *Rhodobacter capsulatus*; Rs, *Rhodobacter sphaeroides*. Genes with no source abbreviation are derived from *Escherichia coli*.

[a] TE represents 17 different *E. coli* genes individually harbored on the ASKA library plasmids (shown as follows): *fadM, ydiI, yciA, ybgC, ybfF, ypfH, tesA, tesB, ybaC, yjfP, bioH, ybdB, frsA, paaI, paaY, yeiG, yqiA*.

[b] PaaI* D16 and H52 saturated mutants were cloned onto the same backbone as wild type.

125 mL Narrow Mouth Erlenmeyer Flask with Phenolic Screw Cap (4985-250/125); vessel 5, 6, 7 are BD Vacutainer Serum Tubes (BD 367820). In the case of Figs. 3B and 6, glucose was fed to the production culture every 12 h (8 g/L for the first 24 h, then 5 g/L afterwards) with adjustment of culture pH to 7.2 using 10M NaOH or 5M KOH:$NH_4OH$ (1:2, v/v, Fig. 6B). For long-term production on Fig. 6B using concentrated cells, the inoculated cultures were first grown at 37 °C to exponential phase then induced for 4 h at 30 °C using the same vessel and condition as described for Fig. 4. Next, the induced cells were spun down and resuspended with 20 mL fresh TB 2% glucose medium to an initial $OD_{600}$ of about 8, then allowed to produce in 125 mL screwed-cap flasks (PYREX 4985-125) for the next few days at 30 °C and 200 rpm.

### 4.4. Protein purification

Protein purification was performed using the His-Spin Protein Miniprep Purification kit from Zymo Research (Irvine, CA). Overnight culture of the XL-1 strains harboring the target enzyme was used to inoculate 20 mL of fresh LB with appropriate antibiotics. The culture was incubated at 37 °C then induced with 0.1 mM IPTG once reaching exponential phase. The induced culture was switched to 30 °C for protein expression. After 18–24 h, the culture was harvested by centrifugation and the resulting pellet was resuspended with 1 mL of His binding buffer suppled in the kit. The resuspended culture was mixed with 1 mL of 0.1 mm glass beads (Biospec) and homogenized using MiniBeadBeater-16, model 607 (Biospec). The soluble fraction was collected by centrifugation at 4 °C. The supernatant was run through the His-binding column, washed and eluted with buffer according to the Zymo protocol. The purified protein was mixed with glycerol for storage at −80 °C. The protein concentration was determined using Bradford reagent with BSA as standards.

### 4.5. In vitro itaconate production using purified enzymes

The reaction mixture contained 100 mM pyruvate, 2.5 mM acetyl-CoA, 100 mM succinate, 5 mM DTT, 5 mM $MgCl_2$, and 0.5 μM of each purified enzyme in the 0.1 M MOPS-KOH buffer (pH 7.0). Reactions were terminated at various time points by adding 1M HCl. Protein debris was removed by centrifugation then 10M NaOH was added to neutralize the samples to pH 7 for HPLC analysis.

### 4.6. Preparation of CoA intermediates

Due to the unavailability of commercial itaconyl-CoA and (S)-citramalyl-CoA, enzymatic synthesis of these two CoA intermediates was performed using purified YpIct and PaIch. To synthesize itaconyl-CoA (reaction A), the reaction mixture contained 1 or 2 mM acetyl-CoA, 10 mM itaconate and 0.025 g/L YpIct in 0.1 M MOPS-KOH buffer (pH 7). After incubation at 30 °C for 30 min (or various time points as shown on Fig. 5), the reaction was terminated by adding 10M HCl to pH around 1. Protein debris was removed by centrifugation at 4 °C followed by pH neutralization to 7 using 10M NaOH. To synthesize (S)-citramalyl-CoA (reaction B), reaction A mentioned above after termination and neutralization was further mixed with 0.025 g/L of PaIch to convert itaconyl-CoA into (S)-citramalyl-CoA. It was later noticed that the preparation of (S)-citramalyl-CoA was equally well achieved by adding YpIct and PaIch simultaneously to reaction A and was chosen as the final preparation method. The reactions were terminated and neutralized using same procedure as mentioned above. The resulting samples were run through Nanosep columns (Pall Life Sciences) then analyzed using HPLC for the different CoA intermediates. Chromatogram peaks corresponding to itaconyl-CoA and (S)-citramalyl-CoA were identified by examining their respective increase and/or decrease in peak area as the target reaction proceeded. Concentration of the synthesized itaconyl-CoA was estimated using the acetyl-CoA absorbance/concentration standard curve and the respective decrease of the acetyl-CoA peak in reaction A. Similarly, concentration of the synthesized (S)-citramalyl-CoA was estimated using the itaconyl-CoA standard curve and the respective decrease of the itaconyl-CoA peak in reaction B. It is noted that certain degree of spontaneous dissociation of CoA from itaconyl-CoA and acetyl-CoA was observed and was subtracted during the calculation of itaconyl-CoA standard curve and kinetic assay of PaaI.

### 4.7. Kinetics assay

*E. coli* PaaI activity towards different CoA intermediates was assayed using HPLC by monitoring the decrease of the respective acyl-CoA peak. The reaction A or B mixture obtained from itaconyl-CoA or (S)-citramalyl-CoA preparation was mixed with 0.1 M KCl and purified PaaI (0.02–0.04 g/L). The initial acyl-CoA substrate concentration were as follows: 1 mM acetyl-CoA (commercial), 0.5 mM itaconyl-CoA (estimated from preparation), or 0.8 mM (S)-citramalyl-CoA (estimated from preparation). The reaction was initiated with the addition of PaaI and allowed to proceed at 30 °C. At various time points, the reaction was terminated by adding 10M HCl to pH around 1. Protein debris was removed by centrifugation at 4 °C followed by pH neutralization to 7 using 10M NaOH. The resulting samples were analyzed using HPLC.

YpCcl activity towards pyruvate and acetyl-CoA was also assayed using HPLC by monitoring the decrease of the acetyl-CoA peak. The reaction mixture contained 10 mM pyruvate, 1 mM acetyl-CoA and purified YpCcl (0.025 g/L) in 0.1 M MOPS-KOH buffer (pH 7). The reaction was terminated and analyzed using the same procedure as described above.

### 4.8. Quantification of metabolites

The amount of itaconate, glucose, and other organic acids were quantified using an Agilent 1260 HPLC equipped with an auto-sampler and an Agilent Hi-Plex H column (5 mM $H_2SO_4$, 0.6 mL/min, column temperature at 50 °C). Glucose was measured with refractive index detector while organic acids were detected using a photodiode array detector at 210 nm. For the identification and analysis of free CoA and CoA esters, Shimadzu Prominence-i LC-2030C 3D Plus HPLC equipped with a GL Sciences C18 column (50 mM $KH_2PO_4$ at pH 5.3 and methanol (9:1, v/v), 1 mL/min, column temperature at 40 °C) was used. Detection was performed at 259 nm and concentrations were determined by extrapolation from standard curves.

### 4.9. Limiting step assay using YpCcl and PaIch

The reaction mixture contained 100 mM pyruvate, 2 mM acetyl-CoA, 5 mM DTT, and 5 mM $MgCl_2$ in 0.1 M MOPS-KOH (pH 7). Purified YpCcl and PaIch were added at 1 or 3 μM as indicated by the ratio “1” or “3”. The reaction was allowed to proceed at 30 °C for 30 min then terminated using the same procedure as described under kinetics assay. Samples were analyzed by HPLC for the resulting itaconyl-CoA and (S)-citramalyl-CoA concentrations.

## CRediT authorship contribution statement

**Ryan S. Wang:** Writing – original draft, Validation, Methodology, Investigation, Formal analysis, Data curation. **Siang-Wun Siao:** Methodology, Investigation, Formal analysis, Data curation, Conceptualization. **Jessica C. Wang:** Validation, Investigation. **Patrick Y. Lin:** Validation, Investigation. **Claire R. Shen:** Writing – review & editing, Writing – original draft, Validation, Supervision, Methodology, Investigation, Funding acquisition, Conceptualization.

## Declaration of competing interest

The authors declare that they have no known competing financial interests or personal relationships that could have appeared to influence

the work reported in this paper.

## Data availability

Data will be made available on request.

## Acknowledgments

This work was supported by the National Science and Technology Council with grant NSTC111-2221-E007-007-MY3 and MOST105-2628-E007-014-MY3.

## Appendix A. Supplementary data

Supplementary data to this article can be found online at https://doi.org/10.1016/j.mec.2024.e00246.

## References

Atsumi, S., Cann, A.F., Connor, M.R., Shen, C.R., Smith, K.M., Brynildsen, M.P., Chou, K. J., Hanai, T., Liao, J.C., 2008a. Metabolic engineering of Escherichia coli for 1-butanol production. Metab. Eng. 10, 305–311.

Atsumi, S., Hanai, T., Liao, J.C., 2008b. Non-fermentative pathways for synthesis of branched-chain higher alcohols as biofuels. Nature 451, 86. U13.

Cantu, D.C., Chen, Y.F., Reilly, P.J., 2010. Thioesterases: a new perspective based on their primary and tertiary structures. Protein Sci. 19, 1281–1295.

Clomburg, J.M., Vick, J.E., Blankschien, M.D., Rodríguez-Moyá, M., Gonzalez, R., 2012. A synthetic biology approach to engineer a functional reversal of the β-oxidation cycle. ACS Synth. Biol. 1, 541–554.

Corma, A., Iborra, S., Velty, A., 2007. Chemical routes for the transformation of biomass into chemicals. Chem. Rev. 107, 2411–2502.

Datsenko, K.A., Wanner, B.L., 2000. One-step Inactivation of Chromosomal Genes in Escherichia coli K-12 Using PCR Products, vol. 97. Proceedings of the National Academy of Sciences, pp. 6640–6645.

De Mey, M., De Maeseneire, S., Soetaert, W., Vandamme, E., 2007. Minimizing acetate formation in E. coli fermentations. J. Ind. Microbiol. Biotechnol. 34, 689–700.

Erb, T.J., Frerichs-Revermann, L., Fuchs, G., Alber, B.E., 2010. The apparent malate synthase activity of rhodobacter sphaeroides is due to two paralogous enzymes, (3)-malyl-coenzyme A (CoA)/β-Methylmalyl-CoA lyase and (3)-malyl-CoA thioesterase. J. Bacteriol. 192, 1249–1258.

Flamholz, A., Noor, E., Bar-Even, A., Milo, R., 2012. eQuilibrator-the biochemical thermodynamics calculator. Nucleic Acids Res. 40, D770–D775.

Gibson, D.G., Young, L., Chuang, R.-Y., Venter, J.C., Hutchison, C.A., Smith, H.O., 2009. Enzymatic assembly of DNA molecules up to several hundred kilobases. Nat. Methods 6, 343–345.

Harder, B.J., Bettenbrock, K., Klamt, S., 2018. Temperature-dependent dynamic control of the TCA cycle increases volumetric productivity of itaconic acid production by Escherichia coli. Biotechnol. Bioeng. 115, 156–164.

Huo, Y.X., Cho, K.M., Rivera, J.G.L., Monte, E., Shen, C.R., Yan, Y.J., Liao, J.C., 2011. Conversion of proteins into biofuels by engineering nitrogen flux. Nat. Biotechnol. 29, 346. U160.

Jeon, H.G., Cheong, D.E., Han, Y., Song, J.J., Choi, J.H., 2016. Itaconic acid production from glycerol using Escherichia coli harboring a random synonymous codon-substituted 5 '-coding region variant of the cadA gene. Biotechnol. Bioeng. 113, 1504–1510.

Kitagawa, M., Ara, T., Arifuzzaman, M., Ioka-Nakamichi, T., Inamoto, E., Toyonaga, H., Mori, H., 2005. Complete set of ORF clones of Escherichia coli ASKA library (a complete set of E. coli K-12 ORF archive): unique resources for biological research. DNA Res. 12, 291–299.

Kotowska, M., Pawlik, K., 2014. Roles of type II thioesterases and their application for secondary metabolite yield improvement. Appl. Microbiol. Biotechnol. 98, 7735–7746.

Lan, E.I., Liao, J.C., 2012. ATP drives direct photosynthetic production of 1-butanol in cyanobacteria. P Natl Acad Sci USA 109, 6018–6023.

Lan, E.I., Wei, C.T., 2016. Metabolic engineering of cyanobacteria for the photosynthetic production of succinate. Metab. Eng. 38, 483–493.

Liang, K., Shen, C.R., 2017. Engineering cofactor flexibility enhanced 2,3-butanediol production in Escherichia coli. J. Ind. Microbiol. Biotechnol. 44, 1605–1612.

Lu, K.W., Wang, C.T., Chang, H., Wang, R.S., Shen, C.R., 2021. Overcoming glutamate auxotrophy in Escherichia coli itaconate overproducer by the Weimberg pathway. Metab Eng Commun 13, e00190.

Luan, H.H., Medzhitov, R., 2016. Food fight: role of itaconate and other metabolites in antimicrobial defense. Cell Metabol. 24, 379–387.

McMahon, M.D., Prather, K.L.J., 2014. Functional screening and analysis reveal thioesterases with enhanced substrate specificity profiles that improve short-chain fatty acid production in. Appl. Environ. Microbiol. 80, 1042–1050.

Meister, M., Saum, S., Alber, B.E., Fuchs, G., 2005. L-malyl-coenzyme A/β-methylmalyl-coenzyme A lyase is involved in acetate assimilation of the isocitrate lyase-negative bacterium. J. Bacteriol. 187, 1415–1425.

Michelucci, A., Cordes, T., Ghelfi, J., Pailot, A., Reiling, N., Goldmann, O., Binz, T., Wegner, A., Tallam, A., Rausell, A., Buttini, M., Linster, C.L., Medina, E., Balling, R., Hiller, K., 2013. Immune-responsive gene 1 protein links metabolism to immunity by catalyzing itaconic acid production. Proc. Natl. Acad. Sci. U.S.A. 110, 7820–7825.

Ohlemacher, S.I., Xu, Y.Q., Kober, D.L., Malik, M., Nix, J.C., Brett, T.J., Henderson, J.P., 2018. YbtT is a low-specificity type II thioesterase that maintains production of the metallophore yersiniabactin in pathogenic enterobacteria. J. Biol. Chem. 293, 19572–19585.

Okabe, M., Lies, D., Kanamasa, S., Park, E.Y., 2009. Biotechnological production of itaconic acid and its biosynthesis in Aspergillus terreus. Appl. Microbiol. Biotechnol. 84, 597–606.

Otten, A., Brocker, M., Bott, M., 2015. Metabolic engineering of Corynebacterium glutamicum for the production of itaconate. Metab. Eng. 30, 156–165.

Ruetz, M., Campanello, G.C., Purchal, M., Shen, H.Y., McDevitt, L., Gouda, H., Wakabayashi, S., Zhu, J.H., Rubin, E.J., Warncke, K., Mootha, V.K., Koutmos, M., Banerjee, R., 2019. Itaconyl-CoA forms a stable biradical in methylmalonyl-CoA mutase and derails its activity and repair. Science 366, 589. +.

Sasikaran, J., Ziemski, M., Zadora, P.K., Fleig, A., Berg, I.A., 2014. Bacterial itaconate degradation promotes pathogenicity. Nat. Chem. Biol. 10, 371. U82.

Shen, C.R., Lan, E.I., Dekishima, Y., Baez, A., Cho, K.M., Liao, J.C., 2011. Driving forces enable high-titer anaerobic 1-butanol synthesis in Escherichia coli. Appl. Environ. Microbiol. 77, 2905–2915.

Shen, X.L., Mahajani, M., Wang, J., Yang, Y.P., Yuan, Q.P., Yan, Y.J., Lin, Y.H., 2017. Elevating 4-hydroxycoumarin production through alleviating thioesterase-mediated salicoyl-CoA degradation. Metab. Eng. 42, 59–65.

Song, F., Zhuang, Z.H., Finci, L., Dunaway-Mariano, D., Kniewel, R., Buglino, J.A., Solorzano, V., Wu, J., Lima, C.D., 2006. Structure, function, and mechanism of the phenylacetate pathway hot dog-fold thioesterase PaaI. J. Biol. Chem. 281, 11028–11038.

Swarbrick, C.M.D., Nanson, J.D., Patterson, E.I., Forwood, J.K., 2020. Structure, function, and regulation of thioesterases. Prog. Lipid Res. 79.

Tillander, V., Alexson, S.E.H., Cohen, D.E., 2017. Deactivating fatty acids: acyl-CoA thioesterase-mediated control of lipid metabolism. Trends Endocrinol. Metabol. 28, 473–484.

Ye, D.Y., Noh, M.H., Moon, J.H., Milito, A., Kim, M., Lee, J.W., Yang, J.S., Jung, G.Y., 2022. Kinetic compartmentalization by unnatural reaction for itaconate production. Nat. Commun. 13.

Zarzycki, J., Brecht, V., Müller, M., Fuchs, G., 2009. Identifying the missing steps of the autotrophic 3-hydroxypropionate CO2 fixation cycle in Chloroflexus aurantiacus. Proc. Natl. Acad. Sci. U.S.A. 106, 21317–21322.

Zhuang, Z.H., Song, F., Zhao, H., Li, L., Cao, J., Eisenstein, E., Herzberg, O., Dunaway-Mariano, D., 2008. Divergence of function in the hot dog fold enzyme superfamily: the bacterial thioesterase YciA. Biochemistry 47, 2789–2796.